18th International Conference on Renewable Energies and Power Quality
(ICREPQ'20)
Granada, Spain, 1st to 3rd April, 2020
Renewable Energy and Power Quality Journal (RE&PQJ)
ISSN 2172-038 X, Volume No.18, May 2020

Some Heat Transfer Data for a Mannitol Derived Phase Change Material

T. Rocha[1], V. Ferreira[2], A. Magalhães[3] and C. Pinho[4]

[1] Departamento de Engenharia Mecânica
FEUP - Rua Dr. Roberto Frias, s/n, 4200-465 Porto, Portugal
tiago.d.rocha95@gmail.com

[2,3] INEGI - Instituto de Ciência e Inovação em Engenharia Mecânica e Engenharia Industrial
Campus da FEUP - Rua Dr. Roberto Frias, 400, 4200-465 Porto, Portugal
vferreira@inegi.up.pt, amagalhaes@inegi.up.pt

[4] CEFT – DEMEC
Rua Dr. Roberto Frias, s/n, 4200-465 Porto, Portugal
ctp@fe.up.pt

Abstract. Heat transfer data for a commercial mannitol derivative, the Plus ICE A164, were obtained in a setup containing a heat exchanger with a single layer of three vertically placed pipes filled with the phase change material (PCM). This PCM has a fusion temperature about 168 ºC. The experimental procedure used an operating cycle composed by a heating and a cooling process, and the PCM temperature time evolution was measured. From these temperature results, the overall heat transfer coefficient, from the heat transfer fluid, a thermal oil, towards the PCM, was of 350 W/(m^2 K), while the average value for the PCM heat transfer coefficient was of 415 W/(m^2 K).

Key words. Mannitol; Phase change materials; Thermal energy storage; Heat transfer.

1. Introduction

The use of phase change materials (PCM) for thermal energy storage facilitates the use of solar systems even at low solar radiation periods, or the storage of surplus discarded thermal energy, available from any other type of source or plant. The greenhouse heating is a typical situation where this kind of energy storage is rather useful [1]. The application of PCM's in domestic heat water production from solar energy is another [2]. Sioshansi and Denholm [3] analyzed the economic impact of the introduction of a thermal energy storage system in concentrated solar energy plants, while Nithyanandam e Pitchumani [4] carried out a detailed economic analysis of the use of phase change materials in concentrated solar plants. The use of phase change materials (PCM) is an economic advantage as it reduces the number and size of the storage reservoirs [5]. It is a most promising solution because it allows a high storage density and an almost isothermal operation [6]. There are many problems with the PCM's, namely due to their low thermal conductivities, low chemical stability, their corrosion capacity towards the storage reservoir materials and large volume variations associated to the change of phases. But new technological developments on the synthesis of new materials are leading to new future promises [6].
The present study concerns the determination of heat transfer coefficients for the design of a concentrated solar energy plant requiring a PCM thermal energy storage. It is part of a set of experiments, where several PCM's were tested in order to obtain heat transfer values [7-9].

2. Experimental Setup and Operating Procedure

The heating experiments for the phase change material (PCM) under analysis were carried out in a laboratory installation where hot thermal oil, the Therminol 66, transferred heat towards the PCM under analysis, which was placed inside a set of three transversal pipes with a slight slope to the horizontal. Two mass flow rates of the thermal oil were used in the experiments. During the PCM cooling period, the circulating thermal oil was cooled by a water cooled shell and tube heat exchanger. A quick reversal of the operating conditions of the laboratory set-up could easily be achieved, and the heating and cooling cycles of the PCM could be implemented in a straightforward manner. Figure 1 presents a global scheme and a picture of the installation.
During the PCM fusion process the thermal oil was heated in the heater A then it was pumped and sent to the test exchanger D. The Therminol 66 was chosen because

it was intended to be used in a future solar plant operating with the PCM under analysis.

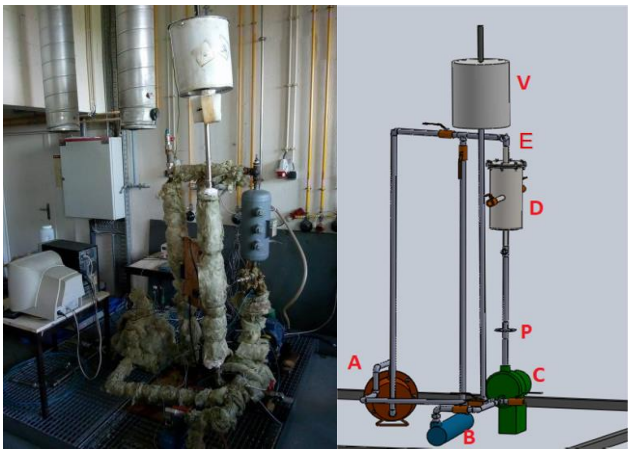

Fig. 1. Picture (left) and scheme (right) of the experimental setup. A - Thermal oil electrical heater; B - Cooling heat exchanger; C- Centrifugal pump; D – Test heat exchanger; E – Air purge; P – Orifice plate flow meter; V – Expansion vessel.

During the PCM solidification step, the thermal oil was cooled in the shell and tube heat exchanger B and then pumped towards the test heat exchanger D. The mass flow rate of the thermal oil was measured by the pressure drop through the orifice plate P, Figure 1. The laboratory installation was equipped with differential pressure transducers and T type thermocouples as necessary to follow the operating process. The computer based data acquisition system is composed by two USB connected interface boards from Measurement Computing and their operation was controlled by the DASYLab software.

3. The Phase Change Material

The PCM that was tested has the commercial designation of Plus ICE A164, and is an alcoholic sugar derived from mannitol ($C_6H_{14}O_6$). The properties supplied by the manufacturer are presented in Table 1. Trhlikova et al. [10] carried out measurements of the thermal properties of this PCM through a ramp-wise and step-wise transient method, and some of the obtained properties are presented in Table 2 for three temperature values.

Table I. - Properties of Plus ICE A164 as supplied by the manufacturer

Phase change temperature, ºC	*Density, kg/m³*	*Latent heat, kJ/kg*	*Specific heat, kJ/(kg K)*	*Specific energy, MJ/m³*
164	1500	290	2.42	435

Table II. - Thermal properties of Plus ICE A164 as determined by Trhlikova et al. [10]

Temperature, ºC	*Phase*	*Thermal diffusivity,* mm²/s	*Thermal conductivity,* W/(m K)	*Specific heat, kJ/(kg K)*
30	solid	0.054	0.06	0.68
100	solid	0.049	0.18	2.45
260	liquid	0.078	0.24	2.07

The mannitol is presented as white powder and its fusion temperature at 1 atm is about 168 ºC. The mannitol is commonly used in the food and pharmaceutical industries and more recently, it was proposed as a thermal energy storage material [11, 12].

Several authors have detected some problems on the mannitol usage as thermal energy storage material. Rodríguez-García et al. [13] indicate that there is a severe degradation of this material when working on thermal energy storage processes when it is subjected to long stages above its fusion temperature. The clear phase change disappears and a vitreous transition phenomenon takes place and from a visual inspection of the degraded material it can be concluded that its solid structure is lost. It is replaced by a brownish pasty structure, typical of a caramelization process. Bayón and Rojas [14] also confirm the caramelization process and have identified a strong volatiles release followed by the polymerization of the solid material. The authors suggest that without a proper stabilization procedure of the material, either through encapsulation or through the formation of a composite structure, this material should not be used for thermal energy storage. Gasia et al. [15] have also detected a serious chemical and thermal degradation of the mannitol after a hundred operation cycles and consequently also refer that the mannitol should not be used as a thermal storage phase change material.

In spite of the above mentioned restrictions, that concern pure mannitol, and not commercially derived mannitol products, the present text discusses the determination of overall heat transfer coefficients in a thermal oil mannitol heat exchanger composed by a single layer of three vertically placed pipes. The thermal oil flows outside at right angles to the three pipes layer while the PCM is inside the tubes. As referred, in the present situation, the mannitol derivative under analysis is a product developed for thermal energy storage applications, the PlusICE A164, and the expectancy was that it would not present such strong degradation of behaviour and properties as found in the pure material. Even so, industrial applications of mannitol derivatives must be carefully evaluated while the aging problems are not solved or minimized.

4. The Test Heat Exchanger

The heat exchanger used in the experiments was composed by a single layer of three almost horizontal pipes. The heat exchanger is made of carbon steel with an internal diameter 159.3 mm and an external diameter of 168.3 mm. There is a bundle of three pipes, which will stay approximately in a perpendicular position towards the external thermal oil crossflow. These pipes have 210 mm length, 48.3 mm of external diameter and 43.1 mm of internal diameter. Figure 2 presents a 3D image of the heat exchanger while in Figure 3 there is a 2D drawing. When placed in the experimental setup this heat exchanger is in a vertically position, Figure 1. In such situation, the transversal pipes have a 5º inclination towards the horizontal to ease the PCM emptying process.

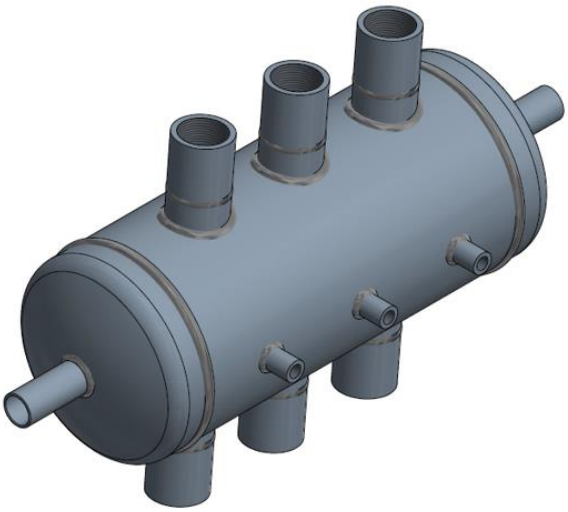

Fig. 2. 3D image of the test heat exchanger.

The external heat transfer area of each pipe is around 0.0241 m^2 and the internal volume of pipe bundle is of 1.348 dm^3.
Figure 3 shows the placement of the thermocouples inside the pipe bundle.

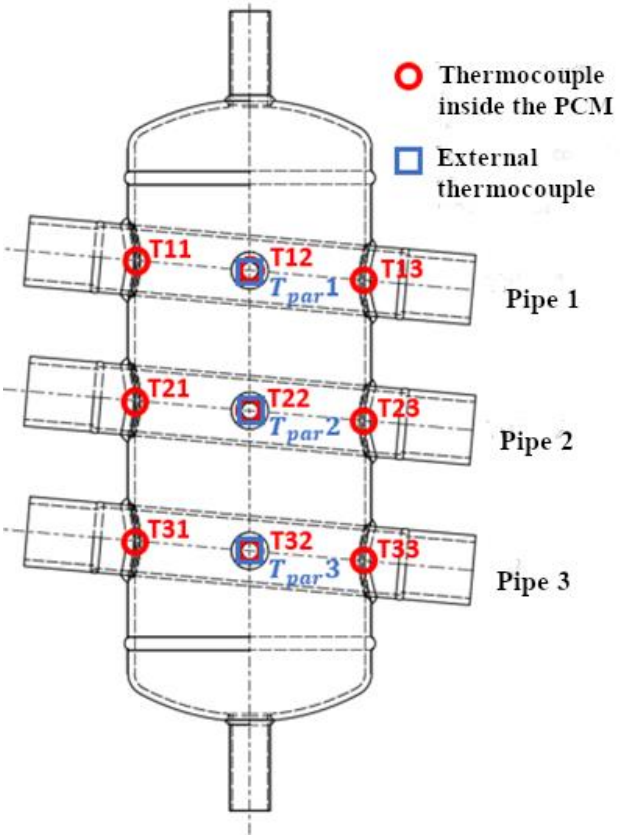

Fig. 3. Test heat exchanger, in its vertical operating position, indicating the location of the inner (red circles) and outer (blue squares) thermocouples.

To evaluate the PCM temperature evolution during the heating and cooling phases, three T type thermocouples were placed inside each one of the pipes. The placement of each thermocouple is indicated by the red circle, Figure 3. Another thermocouple was placed attached to each pipe external wall, this makes easier the determination of the external heat transfer coefficient from the thermal wall towards the pipe inside which there is the PCM. The position of these external thermocouples is also indicated in Figure 3 by means of the blue squares.
Two more T type thermocouples were placed at the heat exchanger inlet and outlet. In this way, the inlet and outlet temperatures of the thermal oil can be continuously monitored.
A total of 1.8 kg of PCM (PlusICE A164), equally distributed by the three pipes, was introduced inside the test heat exchanger. This corresponds to 522 kJ of latent heat of phase change.

5. Heat Transfer Coefficients

Through the application of the First Law of Thermodynamics to the heat exchanger,

$$\dot{Q} = \dot{m}\, c\, \left(T_{ent} - T_{sai}\right) \tag{1}$$

where $\dot{Q}$ is the thermal power supplied by the heat transfer oil in the test heat exchanger, $\dot{m}$ is the thermal oil mass flow rate through the test heat exchanger, c is the specific heat of the thermal oil, T_{ent} is the heat exchanger inlet temperature of the thermal oil and T_{sai} is the heat exchanger outlet temperature of the thermal oil. As the test heat exchanger is well insulated, it can be assumed adiabatic and so the thermal power $\dot{Q}$ supplied by the thermal oil is the thermal power acquired by the PCM inside the three near horizontal tubes,

$$\dot{Q} = U\, A\, \Delta T_{lm} \tag{2}$$

where A is the total heat transfer area, U the overall heat transfer coefficient and ΔT_{lm} is the logarithmic mean temperature difference. Combining the last two equations, the overall heat transfer coefficient is determined through

$$U = \frac{\dot{Q}}{A\, \Delta T_{lm}} = \frac{\dot{m}\, c\, \left(T_{ent} - T_{sai}\right)}{A\, \Delta T_{lm}} \tag{3}$$

During the experiments the thermal oil mass flow rate through the test heat exchanger, as well its inlet and outlet temperatures were registered, the instantaneous thermal being transferred is continuously determined. The mean logarithmic temperature differences are determined with equation (4) as explained in Esteves et al. [8],

$$\Delta T_{lm} = \frac{\left(T_{sai} - T_{PCM}^{final}\right) - \left(T_{ent} - T_{PCM}^{initial}\right)}{\ln\left(\frac{T_{sai} - T_{PCM}^{final}}{T_{ent} - T_{PCM}^{initial}}\right)} \tag{4}$$

The analysis of the experimental data was done for successive time instants and the T_{ent} and T_{sai} values are the average values of the thermal oil for the time interval under consideration. $T_{PCM}^{initial}$ and T_{PCM}^{final} are the initial and

final temperatures of the PCM again for the same time interval [7, 8]. For each one of the pipes the middle thermocouple readings were used because of its position.
For the presentation of the experimental results, the transient initial and final phases were discarded. Data are only shown for the time instants before and after the phase change, as well as the phase change itself. Accordingly, the time evolution of the overall heat transfer coefficient is shown for the above mentioned time instants.
Figures 4 and 5 show the temperature evolution inside the PCM for a pump feeding frequency of 50 Hz. In Figure 6 and 7 it is possible to see the time evolution of the global heat transfer coefficient, in the heating and in the cooling process, respectively, also for a pump feeding frequency of 50 Hz. Looking at the heating process before and after the change of phase, the global heat transfer coefficient diminishes with the temperature increase. This is coherent with the reduction of the PCM heat transfer coefficient, with the temperature increase, as can be seen in Table II. After the change of phase from solid to liquid, the overall heat transfer coefficient has a clear increase, because of the natural convection currents that appear inside the liquid PCM, which leads to a heat transfer increment.
The decomposition of the overall heat transfer coefficient U in its components is given by equation (5) [16]. In this equation, r_{ext} is the external radius of the pipe, r_{int} is the internal radius of the pipe, k is the thermal conductivity of the pipe material, h_{ext} is the external or thermal fluid side, heat transfer coefficient and h_{int} is the internal or phase change material side, heat transfer coefficient.

$$U = \left[\frac{r_{ext}}{r_{int} h_{int}} + \frac{r_{ext} \ln\left(\frac{r_{ext}}{r_{int}}\right)}{k} + \frac{1}{h_{ext}} \right]^{-1} \quad (5)$$

The internal or PCM heat transfer coefficient h_{int} can be calculated from the equation (5) after the overall heat transfer coefficient U and the external or thermal oil heat transfer coefficient h_{ext} are known.

6. Results

The results for the experiments carried out with the three pipes heat exchanger are presented and discussed. Two thermal oil pump velocities were used, to achieve such conditions two electrical feeding frequencies were used. Every experiment includes the full heating and cooling cycle, according to the pump electrical feeding frequency.

Table III. - Average thermal oil mass flow rate and the corresponding Reynolds numbers

Frequency [Hz]	Process	$\dot{m}$ [kg/s]	Re_D
35	Heating	0.426	1022
	Cooling	0.340	61
50	Heating	0.600	1460
	Cooling	0.490	75

Table III shows the average thermal oil mass flow rate for the heating and cooling phase for each operating cycle, according to the pump feeding frequency and the corresponding Reynolds number based on the external pipe diameter.
The equation used for the determination of the Reynolds number assumes that there are no interfering surfaces adjacent to the heat transfer transversal pipes, which is not rigorously correct in the present situation. The transversal pipes are inside a cylindrical container whose inner walls are quite close to the heat transfer pipes. The application of such equation is thus a simplifying approach.

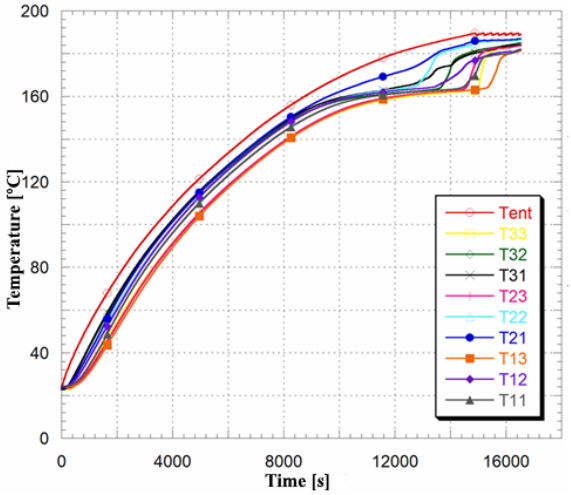

Fig. 4. Time evolution of the PCM temperature during the heating process for a pump feeding frequency of 50 Hz.

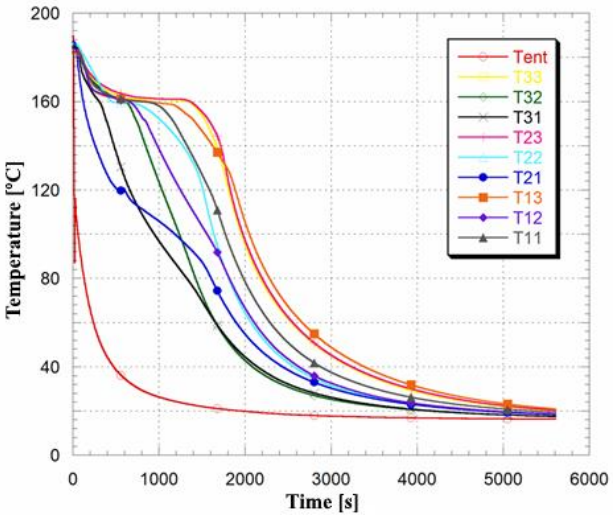

Fig. 5. Time evolution of the PCM temperature during the cooling process for a pump feeding frequency of 50 Hz.

Looking at the plots of Figures 6 and 7 the conclusion is that during the PCM heating step, before and during the phase change the global heat transfer coefficient reduces with the temperature increase because the PCM thermal conductivity diminishes when its temperature increases, as shown in Table II. After the phase change, the global heat transfer coefficient suffers a slight increase, promoted by the natural convection currents taking place inside the melted PCM.

Initially, in the cooling step, the overall heat transfer coefficient is high as all the PCM is in the liquid phase and the natural convection phenomena have a dominant role in the heat transfer process. Closing to the final cooling stage the percentage of PCM in the solid phase is dominant and the overall heat transfer coefficient takes more stable and lower values.

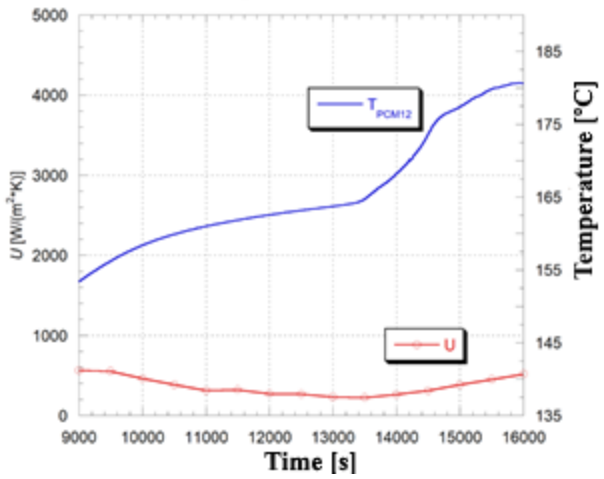

Fig. 6. Time evolution of the global heat transfer coefficient for a pump feeding frequency of 50 Hz, heating process.

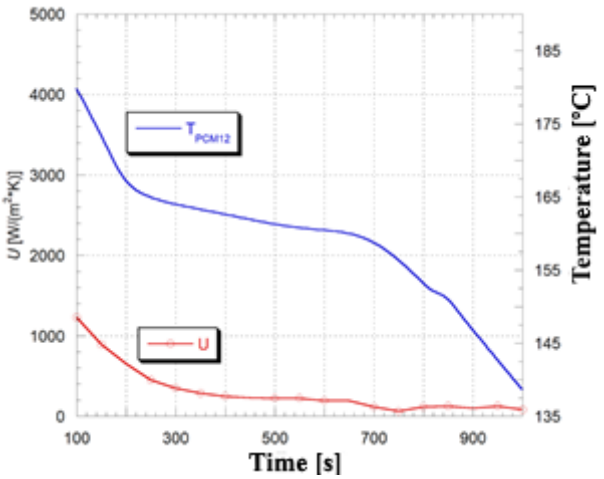

Fig. 7. Time evolution of the global heat transfer coefficient for a pump feeding frequency of 50 Hz, cooling process.

The thermal oil side heat transfer coefficient can be determined through a thermal energy balance between the thermal oil and the external wall of the heat transfer pipes.

$$h_{ext} = \frac{\dot{Q}}{A_{ext}\left(T_{ent} - T_{par}\right)} \qquad (6)$$

A_{ext} is the external surface area of each pipe in contact with the thermal oil, T_{ent} is the inlet temperature of the thermal oil in the test heat exchanger and T_{par} is the pipe external wall temperature. As this external pipe temperature is different for each pipe, there are three evolutions for the external heat transfer coefficient, for each experiment.

Another way to determine the external heat transfer coefficient is through the correlations available in the scientific literature. In the present situation the Zukauskas correlation, as suggested by Incropera et al. [16] was used. Both approaches were used in the present study.

Table IV. - Average values for the global heat transfer coefficient.

Pump feeding frequency [Hz]	Process	Thermocouple	Average global heat transfer coefficient [W/(m²K)]
35	Heating	T_{PCM12}	297
		T_{PCM22}	466
		T_{PCM32}	341
	Cooling	T_{PCM12}	357
		T_{PCM22}	339
		T_{PCM32}	361
50	Heating	T_{PCM12}	354
		T_{PCM22}	354
		T_{PCM32}	398
	Cooling	T_{PCM12}	300
		T_{PCM22}	289
		T_{PCM32}	302

The use of this correlation in the present study is open to doubt as the inner walls of the test heat exchanger might interfere with the thermal oil flow, in other words, the thermal oil flow externally to the transversal pipes cannot be considered a true free external flow. However, from the equations available in the literature this one is the most adequate for the present situation.

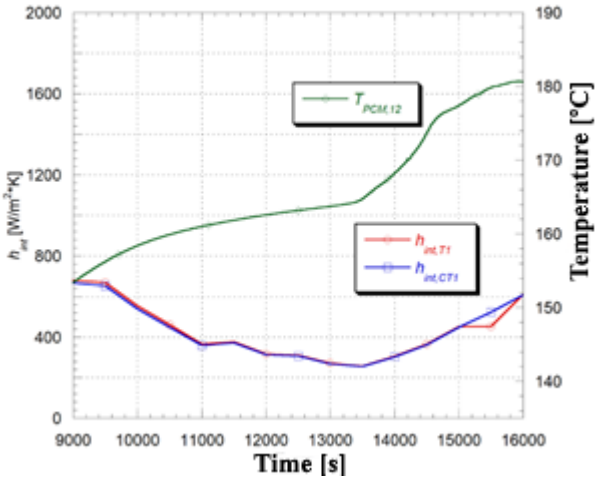

Fig. 8. Time evolution of the PCM heat transfer coefficient for a pump feeding frequency of 50 Hz during the heating process.

Known the overall heat transfer coefficient and the external heat transfer coefficient, it is now easy to determine, the PCM heat transfer coefficient, through equation (5). Figures 8 and 9 show the time evolutions of the PCM heat transfer coefficient, in the heating and cooling steps, for a pump feeding frequency of 50 Hz. It is quite clear that the time evolution of the heat transfer coefficient of the PCM, is independent, from the methodology used in the determination of the heat

transfer coefficient of the thermal oil. This occurs because of the highest heat transfer resistance of the PCM, which dominates the transfer process.

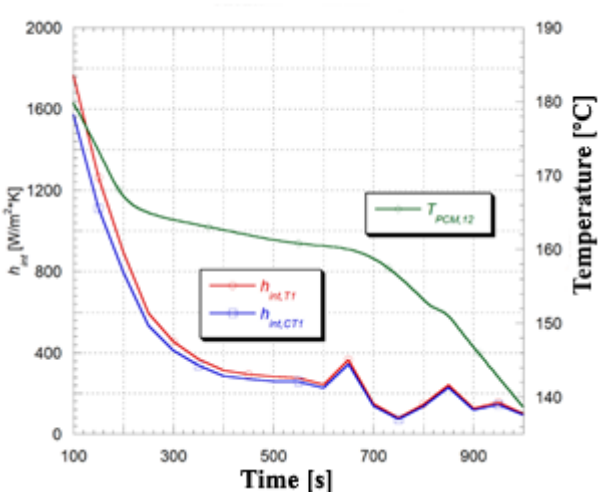

Fig. 9. Time evolution of the PCM heat transfer coefficient for a pump feeding frequency of 50 Hz, during the cooling process.

Table V shows average values for the overall heat transfer coefficient $\bar{U}$ and for the PCM heat transfer coefficient $\bar{h}_{int}$. The values referred by the term "correlation" refer to the values obtained using the external oil heat transfer coefficient, determined by the Zukauskas correlation, while the values referred by the term "experimental", were determined from the knowledge of the external heat transfer coefficient calculated by means of equation (6).

Table V. - Average values for the PCM heat transfer coefficient.

Process	Pipe	$\bar{U}$ [W/(m²K)]	$\overline{h_{int}}$ [W/(m²K)]	
			Correlation	Experimental
Heating 35 Hz	1	297	342	353
	2	466	550	546
	3	341	399	394
Cooling 35 Hz	1	357	432	480
	2	339	411	411
	3	361	440	434
Heating 50 Hz	1	354	406	412
	2	354	406	406
	3	398	464	458
Cooling 50 Hz	1	300	359	397
	2	289	345	345
	3	302	361	359

7. Conclusions

The performance of a PCM, a mannitol derivative with the commercial designation of Plus ICE A164, was analysed in a small test heat exchanger composed by a single layer of three horizontal pipes. Using an operating cycle composed by a heating and cooling process an average value of 350 W/(m² K), for the overall heat transfer coefficient, was determined. Subsequently an average heat transfer coefficient of 415 W/(m² K) for the PCM material was also determined. The time evolution of the PCM heat transfer coefficient is independent from the methodology used for the determination of the external heat transfer coefficient of the pipes containing the PCM.

Acknowledgement

The authors are tankful to the project SHIP (Compete 2020 and Portugal 2020) for the financial support of this work.

References

[1] Öztürk, H.H. 2005. Experimental evaluation of energy and exergy efficiency of a seasonal latent heat storage system for greenhouse heating. Energy Conversion and Management 46: 1523–42.

[2] Solé, C., Medrano, M., Castell, A., Nogués, M. e Cabeza, L. 2007. Energetic and exergetic analysis of a domestic water tank with phase change material. International journal of energy research 31: 135–47.

[3] Sioshansi, R. e Denholm, P. 2010. The value of concentrating solar power and thermal energy storage. Nrel-Tp-6a2-45833 1: 173–83.

[4] Nithyanandam, K. e Pitchumani, R. 2014. Cost and performance analysis of concentrating solar power systems with integrated latent thermal energy storage. Energy 64: 793–810.

[5] Fleischer, A.S. 2015. Thermal Energy Storage Using Phase Change Materials Fundamentals and Applications. Springer. Minneapolis, MN, USA.

[6] Khan, Z., Khan, Z. e Ghafoor, A. 2016. A review of performance enhancement of PCM based latent heat storage system within the context of materials, thermal stability and compatibility. Energy Conversion and Management 115: 132–58.

[7] Esteves, L. P., Magalhães, A., Ferreira, V. and Pinho, C. 2017. Evolution of Global Heat Transfer Coefficient on PCM Energy Storage Cycles. Energy Procedia 136 (2017) 188–195, 4th International Conference on Energy and Environment Research, ICEER 2017, 17th to 20th July 2017, Porto, Portugal.

[8] Esteves, L., Magalhães, A., Ferreira, V. and Pinho, C. 2018. Test of Two Phase Change Materials for Thermal Energy Storage. Determination of the Global Heat Transfer Coefficient. ChemEngineering, 2018, 2(1), 10.

[9] Trindade, J., Magalhães, A, Ferreira, V. and Pinho, C. 2018. Temperature Evolution Inside a Capsule Containing Phase Change Material. ENCIT2018 - 17th Brazilian Congress of Thermal Sciences and Engineering, 25th to 28th November 2018, Águas de Lindóia, SP, Brazil.

[10] Trhlikova, L., Zmeskal, O., Prikryl, R. and Florian, P. 2015. Thermal Properties of Mannitol Derivative. Advanced Materials Research 1126: 181–86.

[11] Oró, E., Gil, A., Miró, L., Peiró, G., Álvarez, S. and Cabeza, L.F. "Thermal energy storage implementation using phase change materials for solar cooling and refrigeration applications". Energy Procedia, 30 (2012), p. 947-956.

[12] Solé, A., Neumann, H., Niedermaier, S., Martorell, I., Schossig, P. and Cabeza, L.F. "Stability of sugar alcohols as PCM for thermal energy storage". Solar Energy Materials & Solar Cells, 126 (2014), p. 125-134.

[13] Rodríguez-García, M.M., Bayón, R. and Rojas, R. 2016. Stability of D-mannitol upon melting/freezing cycles under controlled inert atmosphere. Energy Procedia 91: 218–225.

[14] Bayón, R. and Rojas, E. 2017. Feasibility study of D-mannitol as phase change material for thermal storage. AIMS Energy 5: 404–24.

[15] Gasia, J., Martin, M., Solé, A., Barreneche, C. and Cabeza, L. 2017. Phase Change Material Selection for Thermal Processes Working under Partial Load Operating Conditions in the Temperature Range between 120 and 200 °C. Applied Sciences: 722.

[16] Incropera, F.P., Dewitt, D.P., Bergman, T.L. and Lavine, A.S. 2011. Fundamentals of heat and mass transfer. John Wiley & Sons. USA.